electronics

MDPI

Article

An Active Power Coordination Control Strategy for AC/DC Transmission Systems to Mitigate Subsequent Commutation Failures in HVDC Systems

Xia Zhou [1,*], Cangbi Ding [2], Jianfeng Dai [2], Zhaowei Li [3], Yang Hu [3], Zhaohui Qie [3] and Feng Xue [3]

[1] Institute of Advanced Technology, Nanjing University of Post and Telecommunication, Nanjing 210023, China
[2] College of Automation, College of Artificial Intelligence, Nanjing University of Post and Telecommunication, Nanjing 210023, China; dcb19960926@163.com.cn (C.D.); daijianfeng2012@126.com (J.D.)
[3] NARI Group (State Grid Electric Power Research Institute), Nanjing 211106, China; lizhaowei1@sgepri.sgcc.com.cn (Z.L.); hooyoung@neepu.edu.cn (Y.H.); qiezhaohui@outlook.com (Z.Q.); xue-feng@sgepri.sgcc.com.cn (F.X.)
* Correspondence: zhouxia@njupt.edu.cn; Tel.: +86-13-81-39-00-451

Abstract: Subsequent commutation failures (CFs) in HVDC systems will cause large-scale power flow transfer in AC/DC transmission systems and lead to overload risk in HVAC systems. In order to cope with these effects, a power coordination control strategy for the AC/DC transmission system with high-proportion wind power is proposed. Firstly, a model of the AC/DC transmission system considering the large-scale wind farms access is established by analyzing the power transmission characteristics of the AC/DC transmission system with high-proportion wind power, and the power transmission characteristics are analyzed after subsequent CFs. Secondly, the HVDC subsequent CFs can be mitigated by adjusting DC power transmission, while the active power output of the sending-end AC system is reduced by active control of wind turbine generators (WTGs) to reduce the overload risk of the HVAC system. Finally, the proposed power coordination control strategy is simulated and verified based on the established simulation model and actual power grid, and the results show that this strategy can effectively mitigate HVDC's subsequent CFs and reduce the overload risk in HVAC systems.

Keywords: HVDC subsequent commutation failures; AC/DC transmission system; high-proportion wind power; active power coordinated control

Citation: Zhou, X.; Ding, C.; Dai, J.; Li, Z.; Hu, Y.; Qie, Z.; Xue, F. An Active Power Coordination Control Strategy for AC/DC Transmission Systems to Mitigate Subsequent Commutation Failures in HVDC Systems. *Electronics* **2021**, *10*, 3044. https://doi.org/10.3390/electronics10233044

Academic Editor: Ahmed Abu-Siada

Received: 25 October 2021
Accepted: 3 December 2021
Published: 6 December 2021

1. Introduction

The construction of wind power base and thermal power base in China overlap highly in the regional distribution and are far away from the load center, so the power generation mode of concentrated delivery of high-proportion wind power and traditional thermal power is widely used. Meanwhile, the line-commutated converter, high-voltage direct current (LCC-HVDC) system meets the demand of large-capacity, long-distance power transmission in the power generation process of sending-end AC system with high-proportion wind power [1–3]. Combined with the traditional high-voltage alternating current (HVAC) system, the AC/DC transmission system with high-proportion wind power will be an important development trend of the power system [4,5]. However, the HVDC-CF is one of the most typical faults in the AC/DC transmission system [6]; the CF will cause the power of the HVDC system to drop significantly at the same time, and the power flow of the system will be transferred in a large range, resulting in an overload phenomenon in the HVAC system [7,8]. Therefore, how to mitigate the HVDC's subsequent CFs and the large-scale power flow fluctuation in AC/DC transmission systems is an urgent problem to be solved in modern power systems.

There are many studies on control strategies to mitigate HVDC's subsequent CFs at present, which mainly indicate two methods: voltage-dependent current order lim-

iter control (VDCOL) and CF prevention control (CFPREV). VDCOL limits DC current under low voltage conditions and reduces the active power of the HVDC system, thus mitigating the probability of HVDC's subsequent CFs [9,10]; CFPREV can directly increase the commutation margin according to controlling the inverter to trigger in advance and reducing the CF risk [11]. Reference [12] proposed that virtual resistance was added to the control system to improve the control method of VDCOL, and the voltage after the virtual resistance voltage drop was taken as the input quantity of VDCOL. The authors of [13] used a new power electronic equipment called enhanced line-commutated converter (E-LCC), which is able to mitigate HVDC's subsequent CFs because of its fully controlled sub-modules. Reference [14] proposed an extinction angle predictive (EAP) control strategy that estimates the forthcoming commutation stress based on the commutation voltage waveform and ensures a better sensitivity for HVDC commutation voltage distortion. The authors of [15] adjusted the active power of HVDC systems according to the risk prediction results of subsequent CFs, so as to reduce the reactive power demand in the process of HVDC recovery, which can effectively mitigate HVDC's subsequent CFs. However, an HVDC system is often combined with an HVAC system to form an AC/DC transmission system in an actual power grid, so the active power will drop severely if the method of reference [15] is adopted; a CF will occur in the HVDC system, and the phenomenon of power shock will occur in the HVAC system. Meanwhile, the HVDC system cannot recover to the normal power transmission capacity in time, so the HVAC system is in an overload state for a long time [16].

However, there are few research results on the overload phenomenon of HVAC systems in AC/DC transmission systems. Generally, the power flow controller is used to improve the steady-state power flow distribution of AC/DC transmission systems, but the cost is too high, and the construction has great difficulty; in addition, there is no relevant research on the power flow controller on the regulation strategy of power shock in the transient process [17]. Thus, the problem of large-scale power flow transfer may be solved by reducing the active power output of the sending-end AC system in the AC/DC transmission system with high-proportion wind power, for which two methods of its solution can be adopted: generator shedding or thermal power unit frequency modulation. The first method has the problem of over-shedding, which will increase the unnecessary startup and shut-down times of thermal power units and deteriorate the operation state of wind farms [18], resulting in the reduction in relevant economic benefits. The second method has a very limited power regulation effect on the sending-end AC system with high-proportion wind power and cannot effectively deal with the system power flow fluctuation in time. Therefore, it is of great significance to realize the safe and stable operation of AC/DC transmission systems with high-proportion wind power by rapidly and effectively mitigating HVDC's subsequent CFs and efficiently and economically reducing the overload risk of HVAC systems caused by HVDC subsequent CFs.

In order to mitigate HVDC subsequent CFs and reduce the overload risk of the HVAC system, this paper proposes a comprehensive active coordination control strategy for AC/DC transmission systems with high-proportion wind power. The power flow distribution characteristics of the system were analyzed when HVDC subsequent CFs occur, and HVDC subsequent CFs could be mitigated by reducing the active power transmission to improve the reactive power requirements of the HVDC system. Meanwhile, according to the constructed judgment equation of overload risk of the HVAC system, the overload risk of the HVAC system was effectively reduced through two control modes—the active acceleration control of WTG and the pitch angle control in sending-end AC system, with high-proportion wind power—to realize coordinated optimization control of active power of the AC/DC transmission system. Finally, the AC/DC transmission system with high-proportion wind power was built on a simulation platform, and the proposed control strategy was verified by the simulation model and the actual power grid, respectively.

2. Overall Scheme

The renewable energy base and resource demand center are in reverse distribution in China. In particular, wind energy is mainly concentrated in the northwestern region [3], while the local power grid is limited in scale and cannot completely consume the generated wind power resources. Therefore, the sending-end AC system adopts the concentrated delivery mode of high-proportion wind power and conventional thermal power plants in the power system planning and design. On the other hand, with the application advantages of HVDC systems in large-capacity, long-distance transmission projects becoming more obvious, and combined with the traditional HVAC system, the AC/DC transmission system with high-proportion wind power will become an important component of the actual power grid. Taking the energy base in northwestern China as an example, the AC/DC transmission system with high-proportion wind power was built, as shown in Figure 1a.

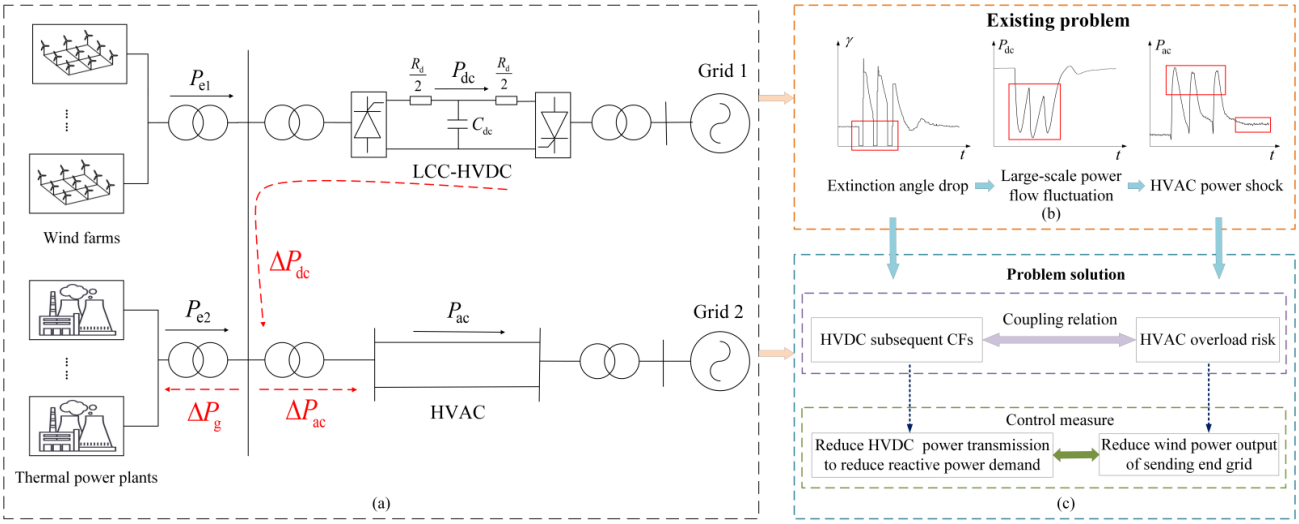

Figure 1. Overall scheme diagram: (**a**) schematic diagram of the AC/DC transmission system with high-proportion wind power; (**b**) existing problem; (**c**) problem solution.

Figure 1b illustrates that the AC-side fault may cause the bus voltage of the inverter side to drop when the receiving-end AC system is connected to the HVDC system. At this time, there will be a CF risk in the inverter station of the HVDC system, which causes the HVDC active power transmission to drop severely and the power flow to transfer widely in the AC/DC transmission system with high-proportion wind power. If the regulation capacity of conventional thermal power plants is limited in the sending-end AC system with high-proportion wind power, an overload phenomenon may occur in the HVAC system.

Since HVDC systems transmit active power mostly, it is necessary to equip the inverter station with reactive power compensation devices to compensate for the reactive power [10]. When the reactive power adjustment capability of the HVDC system is insufficient, HVDC's subsequent CFs can be mitigated by the method of reducing the HVDC active power transmission to reduce reactive power demand. Although this method may cause economic losses, if the HVDC system is faced with locking risk due to subsequent CFs, the economic losses caused by this situation are greater than those caused by the proposed method. In addition, the overload phenomenon will occur in the HVAC system if the regulation capacity of thermal power plants is limited in the sending-end AC system with high-proportion wind power. In order to give full play to the potential of wind farms contributing to the regulation and control of the new power systems, the active power control method in wind power units can be adopted as part of the active power coordination control of the AC/DC transmission system with high-proportion wind power when a CF occurs in

the HVDC system. As shown in Figure 1c, it can reduce the overload risk of the HVAC system, in addition to avoiding the economic and other losses caused by frequent generator shedding of thermal power units in the sending-end AC system.

3. Characteristics Analysis of AC/DC Transmission System with High-Proportion Wind Power

3.1. Analysis of AC/DC Transmission System

LCC-HVDC is composed of the inverter, rectifier, bipolar overhead transmission line, AC/DC filter, reactive power compensation device, flat wave reactor, AC transformer, and other devices, and it has a variety of control modes due to the access of a large number of power electronic equipment, which can improve the operation characteristics and stability of HVDC system.

LCC-HVDC can solve the transmission problem of large-capacity and long-distance in modern power systems, but the HVDC system is only suitable for the transmission mode of two points and one line, and the converter station needs to absorb much reactive power when working, so frequent and timely power regulation cannot be realized. The traditional HVAC system can supply power to the area along the way at the midway point according to the need, and it can be flexibly and automatically adjusted. Therefore, the advantages and disadvantages of HVDC and HVAC systems can be complementary when working together. The advantages of the AC/DC transmission system are mainly reflected in the following three aspects: (1) HVAC and HVDC systems cooperate with each other, so the power supply of the sending-end AC system cannot be sent out due to the failure of a single line, thus enhancing the power supply reliability of the power grid; (2) the reactive power regulation modes of the two can support each other, and the system stability is improved; (3) the HVDC system transmits power exceeding the equivalent distance, while the HVAC system transmits power less than the equivalent distance; thus, it can effectively reduce the investment and operation costs.

3.2. Model and Characteristics of D-PMSG

WTG with variable speed and constant frequency is the mainstream type of WTG technology application at present, an example of which is a directly driven WTG with permanent magnet synchronous generators (D-PMSGs). This model is considered the WTG technology with the most potential for development in the future due to its long service life, convenient maintenance, and high efficiency [19,20]. Therefore, a D-PMSG was selected as the WTG model in the sending-end AC system with high-proportion wind power in this study.

The mechanical power obtained by D-PMSG can be expressed as

$$P_{\mathrm{w}} = \frac{1}{2} C_{\mathrm{p}}(\lambda, \beta) \rho S v^3 \tag{1}$$

where P_{w} is the mechanical power obtained by wind speed on the shaft system of WTG; ρ is the air density; S is the scavenging area of the WTG blade; v is the wind speed; C_{p} is the wind energy utilization coefficient, which is the function of tip speed ratio λ and pitch angle β, and the C_{p} is expressed as

$$C_{\mathrm{p}} = 0.22\left(\frac{116}{\mathrm{b}} - 0.4\beta - 5\right) e^{-\frac{12.5}{\mathrm{b}}} \tag{2}$$

where parameter b and tip speed ratio λ can be expressed as

$$\mathrm{b} = \frac{1}{\frac{1}{\lambda + 0.08\beta} - \frac{0.035}{\beta^3 + 1}} \tag{3}$$

$$\lambda = \frac{w_M R}{v} \tag{4}$$

where w_M is the mechanical angular velocity of the WTG blade, and R is the radius. According to Equation (2), when β is fixed, the C_{P} value changes with the λ; only when λ

is a certain value, the C_P value is the largest, and the system conversion efficiency is the highest point; the blade tip speed ratio is called the optimal blade tip speed ratio λ_{opt} at this time. The speed of the D-PMSG system can be controlled by adjusting the power output so that the D-PMSG system can operate under the state λ_{opt} and maintain the maximum value of C_P when the wind speed changes greatly. At this rate, the problem of conversion efficiency of wind energy to mechanical energy can be solved.

According to the natural characteristic curve of the WTG, the optimal blade tip speed ratio λ_{opt} is taken λ as the input instruction to ensure that the D-PMSG system works at the maximum power point. Maximum power point tracking (MPPT) can be achieved by subsequently adjusting the WTG speed to keep it running at the corresponding optimal speed λ_{opt}, as shown in the blue dotted line in Figure 2.

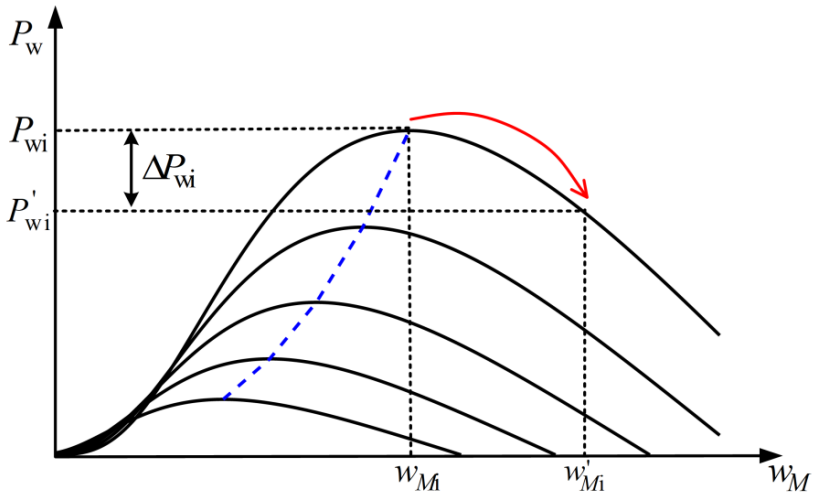

Figure 2. Schematic diagram of active acceleration control of WTG.

The D-PMSG model based on a back-to-back dual PWM converter has a flexible control mode, and the operational characteristics of the system can be enhanced by using the vector control method. The generator-side converter and the grid-side converter have different functions in D-PMSG [21]. The generator-side converter generally adopts rotor flux orientation to make the stator current presents a sinusoidal waveform, and it can realize the rapid adjustment of speed and power factor. The grid-side converter adopts the grid voltage vector orientation and reverses the DC into a qualified sine wave, so as to realize the grid connection and the decoupling of active and reactive power.

3.3. Principle of HVDC Quick Power Drop

The relationship between the extinction angle γ, converter trigger angle α, HVDC active power transmission P_{dc}, the effective value of the converter bus voltage U_L, and other parameters in the HVDC system is as follows:

$$\cos\gamma = -\cos\alpha - \frac{kP_{dc}}{U_L^2\cos\alpha} \tag{5}$$

According to Taylor formula, the first-order expansion of Equation (5) can be obtained as follows:

$$\Delta\gamma = \frac{kP_{dc} - U_L^2\cos^2\alpha}{U_L^2\cos^2\alpha}\Delta\alpha - \frac{2kP_{dc}}{U_L^3\sin\alpha\cos\alpha}\Delta U_L + \frac{k}{U_L^2\sin\alpha\cos\alpha}\Delta P_{dc} \tag{6}$$

The trigger angle α of the inverter station and the effective value U_L of the converter bus voltage generally remain unchanged in practical engineering, and the coefficient of ΔP_{dc} is negative [10]. The extinction angle γ increases with the decrease in HVDC power transmission P_{dc}, which can reduce the probability of CF in the HVDC system. Therefore, the extinction angle can be increased as long as the HVDC power transmission can be

decreased when AC-side fault occurs in the system under the condition that the constant power control and the constant extinction angle control of the HVDC system have all been completed the operation, so as to mitigate HVDC's subsequent CFs. The HVDC system currently in operation is equipped with quick power drop devices, which are generally installed on the HVDC system rectifier side and cooperates with various control devices on the inverter side to realize the effect of the quick power drop in the HVDC system.

4. Influence of HVDC Subsequent CFs on the HVAC System

4.1. Influence Factors of HVDC-CF

CF refers to the phenomenon in which the valve that exited conduction at the end of commutation failed to restore its blocking ability during the period under the action of reverse voltage, or the valve that should have exited conduction failed to exit conduction again under the action of direct voltage in time. Therefore, the essence of CF is that the extinction angle of valve operation is less than its limit. When the AC system on the inverter side runs in a symmetrical state, its extinction angle γ, the effective value of commutation bus voltage U_L, commutation reactance X_c, DC current I_d, advance trigger angle ϑ, and commutation voltage zero-crossing offset angle φ satisfy the following relationship:

$$\gamma = \arccos\left(\frac{\sqrt{2}X_c I_d}{U_L} + \cos\vartheta\right) - \varphi \tag{7}$$

As the first CF occurs quickly and has little influence, it is more in line with the actual demand to pay attention to uncertainty factors of subsequent CFs. It can be seen from Equation (7) that the extinction angle is mainly affected by DC current, converter bus voltage, and advanced trigger angle. The converter bus voltage decreases and the DC current suddenly increases when AC-side failure occurs in the HVDC system At this time, the VDCOL link of the system starts to work, and the current limit order of the VDCOL link cannot immediately be reduced because of the large inductance of the smoothing reactor. It is a process of rising first and then falling, so the converter valve cannot work in time, resulting in subsequent CFs. If subsequent CFs occur in the HVDC system, the system will face the risk of HVDC pole blocking.

4.2. Power Flow Analysis of AC/DC Transmission System

The steady-state power flow distribution of the AC/DC transmission system with high-proportion wind power is shown in the black arrow in Figure 1a. The power output P_e of the sending-end AC system is composed of the active power output P_{e1} from wind farms and the active power output P_{e2} from thermal power plants. The active power transmission on the HVDC system is P_{dc}, and the active power on the HVAC system is P_{ac}.

The drop in active power on the HVDC system will cause severe harm to the AC/DC transmission system when a CF occurs in the HVDC system as an AC-side fault, and this will lead to a large-scale power flow transfer in the system. The amount of active power dropped by the HVDC system will be adjusted by the frequency modulation system of traditional thermal power plants, and the remaining amount will be transferred to the HVAC system, which may lead to the cascading trip of the HVAC system for overload, resulting in a large-scale blackout accident in the power system.

The specific power change is shown in the red dotted line in Figure 1a. The active power of the HVDC system drops severely due to the subsequent CFs, and its active power drop value is set as ΔP_{dc}. Meanwhile, the thermal power plants start the frequency modulation system to reduce the output power ΔP_g. However, the amount ΔP_{dc} that does not contribute to frequency modulation of the thermal power plants will be transferred to the HVAC system due to the limited frequency modulation capability of the thermal power plants; the active power added to the HVAC system is ΔP_{ac}, and an overload phenomenon occurs in the HVAC system.

Therefore, it is necessary to consider the mitigation of subsequent CFs in HVDC systems, as well as the reduction in the HVAC system's overload risk caused by the large-

scale power flow transfer of the system when the HVDC subsequent CFs occur in the AC/DC transmission system with high-proportion wind power.

4.3. Overload Risk of HVAC System

The equivalent circuit diagram of the HVAC system in Figure 1a is shown in Figure 3, where δ_1 is the phase angle difference between the generator terminal voltage E_q and the bus voltage $U_2\angle 0$ of grid B; the voltage of the sending-end AC system is $U_1\angle\theta$; the direct axis reactance of the generator is X_d; X_{T1} and X_{T2} are the equivalent reactance of the transformers on both sides of AC line; X_L is the AC line reactance. The equilibrium power point of the AC/DC transmission system model is expressed as follows:

$$P_\mathrm{dc} = \frac{E_q U_1}{X_\mathrm{d} + X_{T1}} \sin(\delta_1 - \theta) - \frac{U_1 U_2}{X_L + X_{T2}} \sin\theta \tag{8}$$

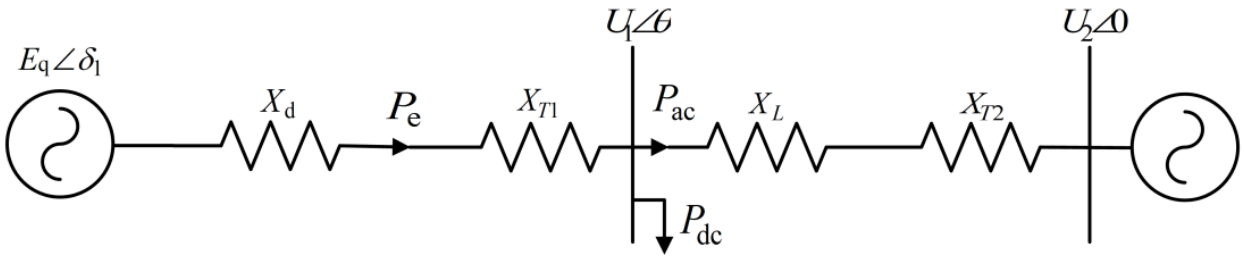

Figure 3. Equivalent circuit diagram of AC/DC transmission system.

After subsequent CFs occur in the HVDC system, the drop value of active power satisfies the following expression:

$$\begin{aligned} \Delta P_\mathrm{dc} &= \Delta P_e + \tfrac{\partial P_\mathrm{dc}}{\partial \delta_1} + \tfrac{\partial P_\mathrm{dc}}{\partial \theta} \\ &= \tfrac{P_\mathrm{dc}}{U_1}\Delta U_1 + \tfrac{E_q U_1}{(X_\mathrm{d}+X_{T1})}\cos(\delta_1-\theta)\Delta\delta_1 - \Delta\theta\left(\tfrac{E_q U_1}{(X_\mathrm{d}+X_{T1})}\cos(\delta_1-\theta) + \tfrac{E_q U_1}{(X_L+X_{T2})}\cos\theta\right) \end{aligned} \tag{9}$$

The power angle relationship of the HVAC system is as follows:

$$P_\mathrm{ac} = \frac{U_1 U_2}{(X_L + X_{T2})} \sin\theta \tag{10}$$

$$\Delta P_\mathrm{ac} = \frac{\mathrm{d}P_\mathrm{ac}}{\mathrm{d}\theta} = \frac{U_1 U_2}{(X_L + X_{T2})} \cos\theta = -K\Delta f_\mathrm{ac} \tag{11}$$

where ΔP_ac is the power variation; $\Delta\delta_1$ is the variation of power angle when AC-side faults occur in the HVDC system; ΔU_1 is the voltage variation of the sending-end AC system; $\Delta\theta$ is the variation of the phase angle between U_1 and U_2; Δf_ac is the frequency variation of the AC system; K is the slope. According to the above analysis, the power shock in the HVAC system is closely related to the power variation in the HVDC system and the active power output of the sending-end AC system.

5. Coordination Control Strategy for the AC/DC Transmission System

5.1. Measure for the Mitigation of HVDC Subsequent CFs by DC Power

The occurrence of HVDC subsequent CFs is closely related to the reactive power of the receiving-end AC system, so the reactive power demand and recovery characteristics of the inverter station during the CF should be analyzed. The steady-state approximate equation of the inverter side is concluded as follows:

$$\begin{cases} \phi = \arccos(U_\mathrm{di}/U_\mathrm{di0}) \\ P_\mathrm{dc} = U_\mathrm{di} I_\mathrm{d} \\ Q_\mathrm{dc} = P_\mathrm{dc}\tan\phi \end{cases} \tag{12}$$

$$\begin{cases} U_{\mathrm{di0}} = \frac{3\sqrt{2}U_L}{k\pi}B \\ U_{\mathrm{di}} = U_{\mathrm{di0}}\frac{(\cos\gamma+\cos\beta)}{2} \end{cases} \tag{13}$$

where P_{dc} and Q_{dc} are active power and reactive power, respectively; ϕ is the power factor of the converter; U_{di} and I_{d} are DC voltage and DC current, respectively; γ is the extinction angle; U_{di0} is the ideal no-load DC voltage; U_L is the effective value of bus line voltage on the high voltage side; k is converter transformer ratio; B is the number of bridges connected in series; X_c is commutation reactance. The active power transmission and reactive power consumption of the HVDC system are obtained by combining Equations (12) and (13) as follows:

$$Q_{\mathrm{dc}} = P_{\mathrm{dc}}\tan\phi = P_{\mathrm{dc}}\sqrt{\frac{4}{(\cos\gamma+\cos\beta)^2}-1} \tag{14}$$

Reducing the DC active transmission power can effectively reduce the reactive power demand during the HVDC subsequent CFs according to Equation (14). According to Equation (7), when the commutation voltage zero-crossing offset angle φ is not considered, the DC current of the system can be expressed as

$$I_{\mathrm{d}} = \frac{U_L}{\sqrt{2}X_c}(\cos\gamma-\cos\beta) \tag{15}$$

The extinction angle γ and the HVDC active power transmission P_{dc} can be obtained after the following relationship is satisfied by combining Equations (12), (13), and (15):

$$P_{\mathrm{dc}} = \frac{3}{2\pi X_c}U_L^2(\cos^2\gamma-\cos^2\beta) \tag{16}$$

If the inverter-side AC voltage remains unchanged, the advance trigger angle β is set as 38° according to the actual system demand, and the active power of the HVDC system can be expressed as

$$P_{\mathrm{dc}} = k(\cos^2\gamma-\cos^2 38) \tag{17}$$

The extinction angle drops to 1.5° as a reference value when a CF occurs in the system, according to Equation (17), and if the DC power drops by 18.5%, the extinction angle can be restored to 15° to reach the value of the system in normal operation. When the DC power drops by 5.2%, the extinction angle increases from 1.5° to 7.2°, reaching the inherent limit value of extinction angle.

5.2. Principle of Active Control of Wind Turbine Generator

The risk of system power flow transfer caused by the HVDC-CF can be reduced by adjusting the active power output of sending-end AC system in the AC/DC transmission system with high-proportion wind power, and the thermal power plants may effectively control the active power output due to its corresponding frequency modulation capability. However, in order to avoid frequent start-up and shut-down of thermal power plants, reduce related economic losses, and enhance the utilization efficiency of wind farms connected to the grid, a coordinated control strategy of active power in AC/DC transmission system is formulated by adjusting the output power of wind farms.

According to Equations (1) and (2), it can be seen that the power obtained by D-PMSG is directly proportional to the wind energy utilization coefficient under the premise that the relevant conditions remain unchanged. The wind energy utilization coefficient C_{p} is a function of tip speed ratio λ and pitch angle β, and tip speed ratio λ can be controlled by adjusting the rotor mechanical angular velocity when the pitch angle is fixed to achieve the purpose of adjusting wind energy utilization coefficient, so the D-PMSG active power output can be regulated effectively.

D-PMSG adopts MPPT working mode when it is in the normal working state, and this means that it works at the position with the highest wind energy utilization coefficient, as shown in Figure 2. The WTG begins to deviate from the optimal tip speed ratio λ_{opt} and drops to λ'_{opt} opt when the mechanical angular velocity of WTG accelerates from

w_{Mi} to w'_{Mi}, so the wind energy utilization coefficient C_p can be changed according to Equations (3) and (4). Thus, the active power output of WTG reduces from P_{wi} to P'_{wi}, and the active power output reduced by active acceleration control of the mechanical angular velocity of the WTG is as follows:

$$\Delta P_{wi} = P_{wi} - P'_{wi} = \frac{1}{2}\rho S v^3 \left(C_{pmax} - C'_p\right) \tag{18}$$

where C'_p can be expressed as

$$\begin{cases} C'_p = 0.22\left(\frac{116}{b'} - 0.4\beta - 5\right)e^{-\frac{12.5}{b'}} \\ b' = \frac{1}{\frac{1}{\lambda'+0.08\beta} - \frac{0.035}{\beta^3+1}} \\ \lambda' = \frac{w'_{Mi}R}{v} \end{cases} \tag{19}$$

In the process of active control to accelerate the mechanical angular velocity of the WTG blade and reduce the active power output, it is necessary to ensure that the mechanical angular velocity of the WTG blade cannot exceed its maximum speed w_{Mmax}.

The pitch angle control mode of D-PMSG is adopted when the command of WTG speed is greater than the maximum speed. This method is to control the blade installed on the hub to adjust the pitch angle and then change the aerodynamic characteristics of the blade to improve the force of both the blade and the whole machine, to adjust the output power and keep it stable at high wind speed.

Therefore, according to the power flow change in the AC/DC transmission system, the active power output of the sending-end AC system with wind farms can be adjusted in time through two control modes of the active acceleration control of WTG and the pitch angle control.

5.3. Overload Control Strategy of HVAC System

Assuming that the power transmission limit of the HVAC system is P_{acl}, the increment of the power transmission limit is ΔP_{acl}, the adjustable active power of the thermal power plants is ΔP_g, and the maximum adjustable active power of it is ΔP_{gmax}. Meanwhile, assuming that the active power loss of the system line is not taken into account, the increase in the active power ΔP_{ac} of the HVAC system is expressed as follows:

$$\Delta P_{ac} = \Delta P_{dc} - \Delta P_{acl} \tag{20}$$

Due to the limit of the frequency modulation ability of traditional thermal power units, the harm of overload phenomenon of the HVAC system will be further enhanced when the high-proportion wind farms connect to the AC/DC transmission system. The method of generator shedding is generally suggested to solve the problem of the overload phenomenon in HVAC systems, but this method is conservative and cannot give full play to the advantages of wind power regulation. Therefore, an active coordination control strategy of active power can be formulated by using the active control method of WTG to adjust the active power output of the sending-end AC system; the control strategy flow is shown in Figure 4.

CORDER is the DC current order of the inverter side of the HVDC control system, while CMRS is the DC current measurement value of the rectifier side; the current deviation $\Delta\varepsilon$ can be obtained by the difference between CORDER and CMRS. The increase in $\Delta\varepsilon$ will bring about an increase in advance trigger angle ϑ, further reducing trigger angle α ($\alpha + \vartheta = 180^\circ$), to realize the active power regulation of the HVDC system and reduce the system reactive power demand; thus, HVDC's subsequent CFs will be mitigated effectively.

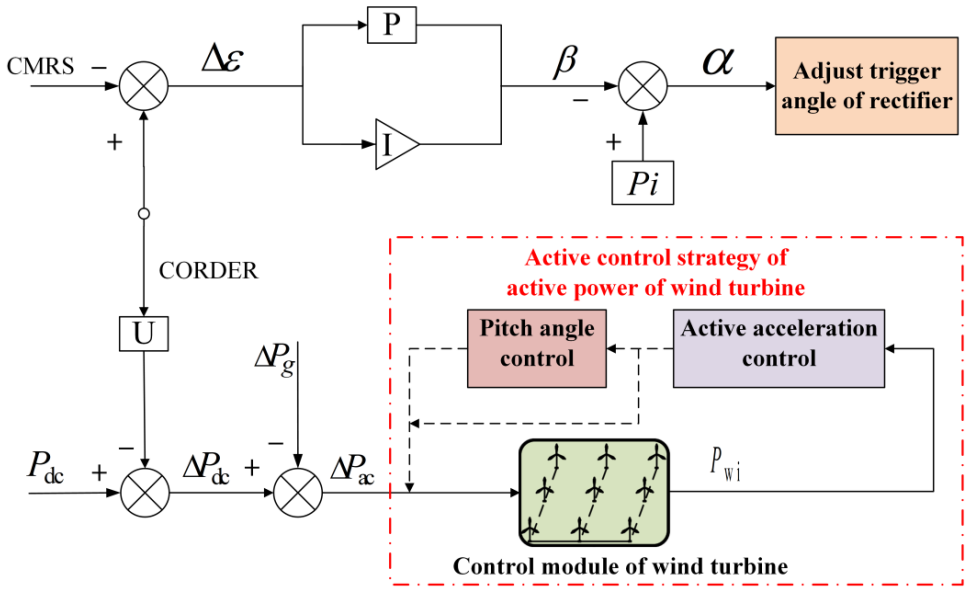

Figure 4. Power coordination control strategy.

If the drop value ΔP_{dc} of HVDC active power transmission cannot be adjusted through the frequency modulation system of thermal power plants completely, that is, the value obtained by Equation (20) is greater than 0, then it is suggested to adopt the active control strategy of wind power proposed in Section 3.2. When the required adjustment amount ΔP_{ac} is input to the control module of WTG, the active acceleration control of WTG is first carried out, and if the active power output of the wind farms can be reduced before the blade reaches the maximum speed $w_{M\max}$, the active control of wind power is completed. If the increase in active power ΔP_{ac} cannot be completely reduced after the WTG reaches the maximum speed $w_{M\max}$, the pitch angle control of WTG starts to work, and the part not regulated by the acceleration control is adjusted. Therefore, the overload risk of the HVAC system can be reduced during the process of HVDC-CF mitigation through the active control strategy of the active power in WTGs.

The proposed strategy can reduce the steady-state overload risk of the HVAC system after the mitigation of HVDC's subsequent CFs, and it can also adjust the transient power shock of the HVAC system during the process of mitigating subsequent CFs in the HVDC system.

To summarize, the flowchart of the control strategy described in this paper is shown in Figure 5.

(1) When the system detects that the first CF occurs, adjust the CORDER from 1 to 0.9 according to Equations (15)–(17). The reactive power demand characteristics of the system can be improved by reducing the active power P_{dc} of the HVDC system;

(2) The large-scale power flow transfer caused by the HVDC-CF should be considered while mitigating HVDC's subsequent CFs. According to Equation (20), the WTG does not need to participate in the active power coordination control of the AC/DC transmission system when $P_{acl} \leq P_{ac} - \Delta P_{g\max}$;

(3) On the premise that the thermal power unit has been fully regulated within the specified range, there will be an overload phenomenon in the HVAC system when $P_{acl} > P_{ac} - \Delta P_{g\max}$. The active control strategy of power of WTG is adopted to reduce the active power output ΔP_{wi}, and let $\Delta P_{Wi} = \Delta P_{ac} - \Delta P_{g\max}$ max according to Equation (18), to reduce the transient and steady-state overload risk of the HVAC system.

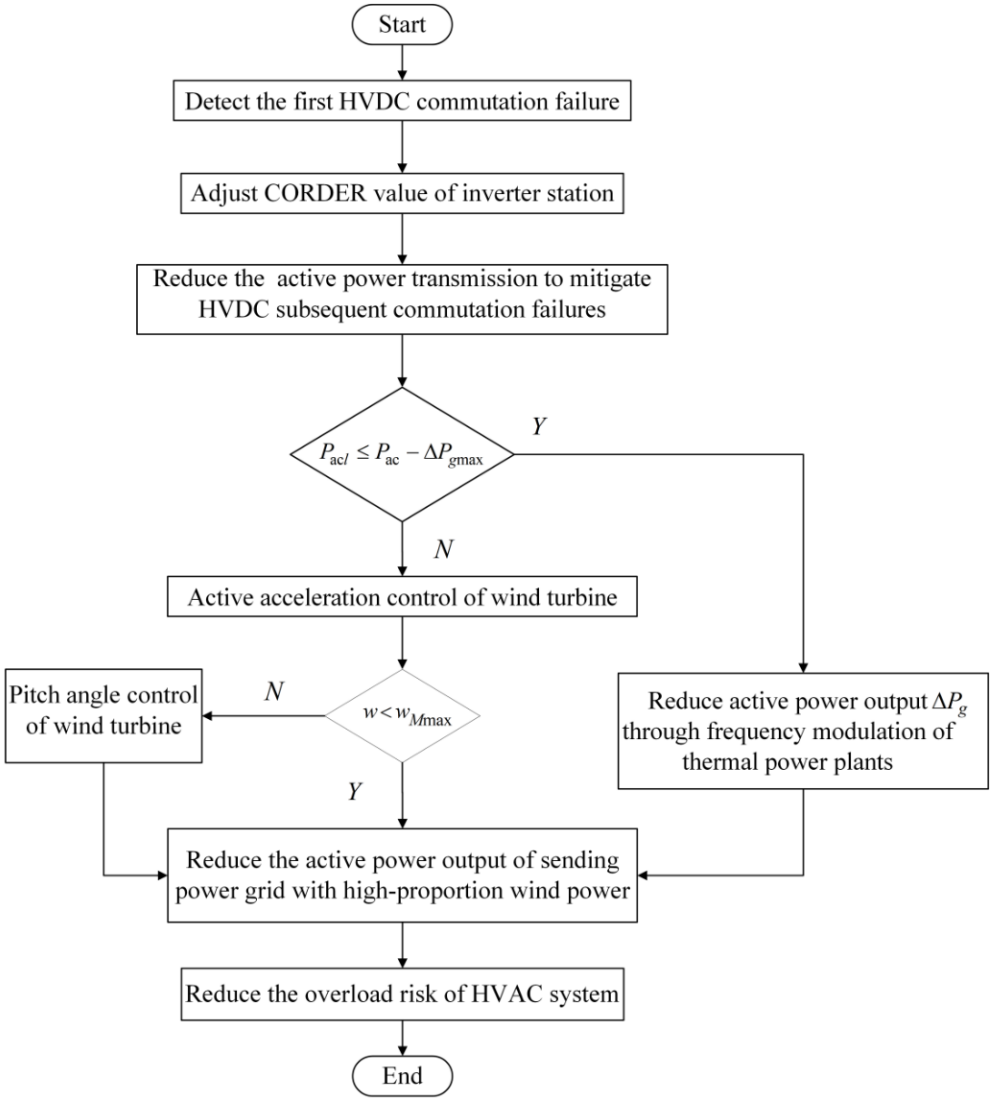

Figure 5. Flowchart of control strategy.

It must be noted that the active power coordination control strategy of the AC/DC transmission system considering HVDC subsequent CFs mitigation proposed in this paper does not fully consider the communication delay in the process of data collection and control instruction delivery, and the application of relevant methods in this control strategy is the focus of follow-up research.

6. Simulation Verification

6.1. Electromagnetic Transient Simulation

The model of an AC/DC transmission system with high-proportion wind power was built, as shown in Figure 1a, in the electromagnetic transient simulation software PSCAD/EMTDC. The rated capacity of wind farms is 1800 MW, and that of thermal power plants is 1200 MW; the voltage level of HVAC system is 330 kV, and the corresponding rated capacity is 1600 MW; the voltage level of the LCC-HVDC system is ±500 kV, and the corresponding rated capacity is 1000 MW; the wind speed of the wind farms is 13 m/s, and the related electrical quantity curve in the normal operation of the system is shown in Figure 6. The active power output of the wind farms is 1240 MW, the HVDC active power transmission is 960 MW, the HVAC active power transmission is 1300 MW, and the

extinction angle of the HVDC system is maintained at 15° [22]. The detailed simulation parameters are presented in Appendix A.

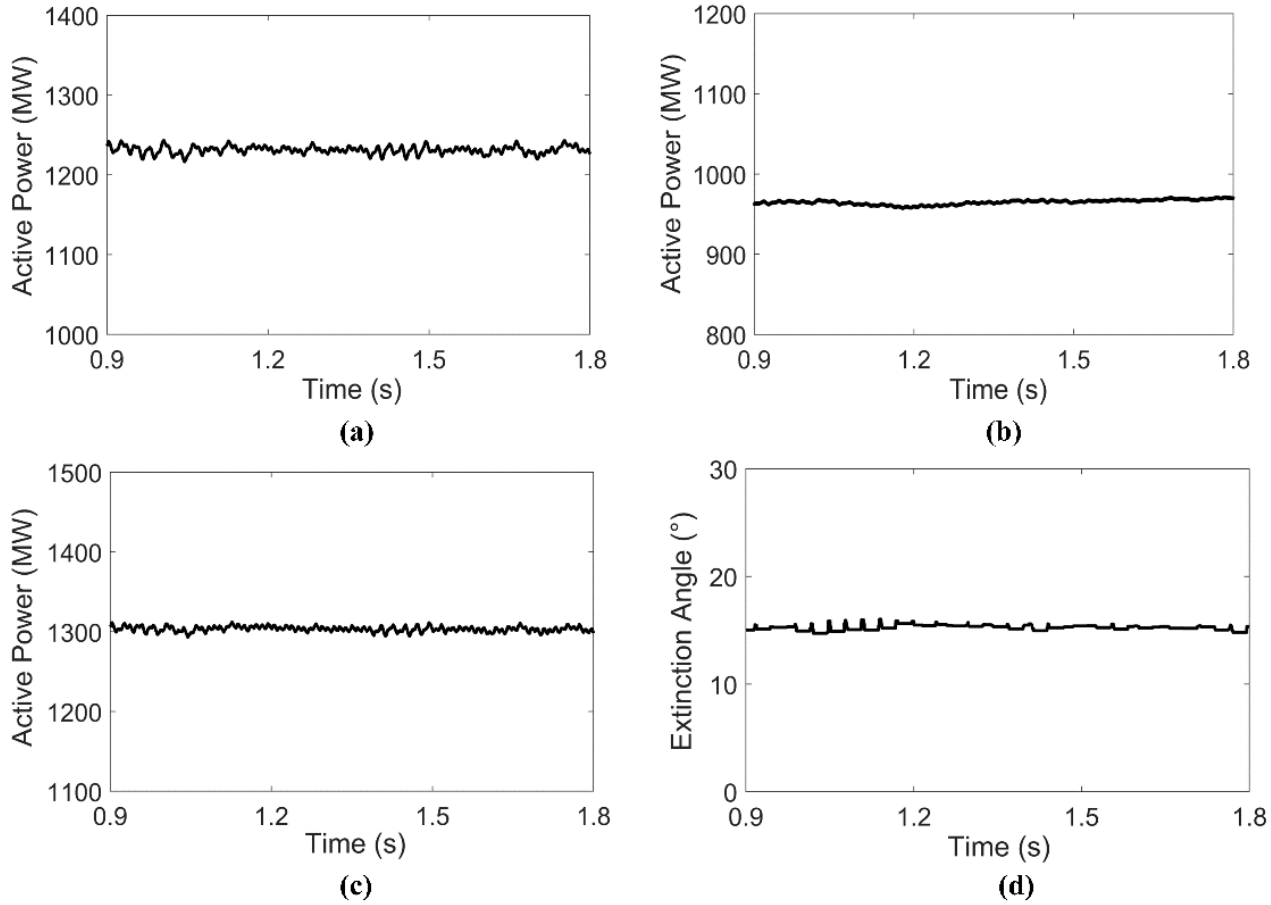

Figure 6. Normal operation characteristics of the AC/DC transmission system with high-proportion wind power: (**a**) active power output of wind farms; (**b**) active power transmission of HVDC system; (**c**) active power transmission of HVAC system; (**d**) extinction angle of HVDC inverter.

A three-phase ground fault was set when the inverter bus of the system operated at 1 s, and the fault duration was 0.05 s. The active power coordination control strategy for the HVDC subsequent CFs mitigation was verified by the following three schemes:

Control scheme 1: CIGRE standard test model control;

Control scheme 2: The HVDC active power transmission was reduced by adjusting the DC current order on the inverter side of the HVDC system, and the reactive power demand of the system was improved;

Control scheme 3: The proposed control strategy in this paper.

When control scheme 1 was adopted, the simulation curves of various electrical quantities were analyzed, shown in the black curve in Figure 7, and whether HVDC-CF occurred in the system was judged by the voltage drop in the converter bus at the inverter side in practical engineering. In the electromagnetic transient simulation, the number of times HVDC-CF can be expressed by observing the number of times of extinction angle drop. As is shown in Figure 7d, the extinction angle drops to 1.5° twice continuously, and the HVDC active power transmission also drops 450 MW twice when subsequent CFs occur in the HVDC system. The HVAC system has two transient power shocks at the same time, during which the peak value reaches 1520 MW, and the system resumes steady-state operation in 1.35 s.

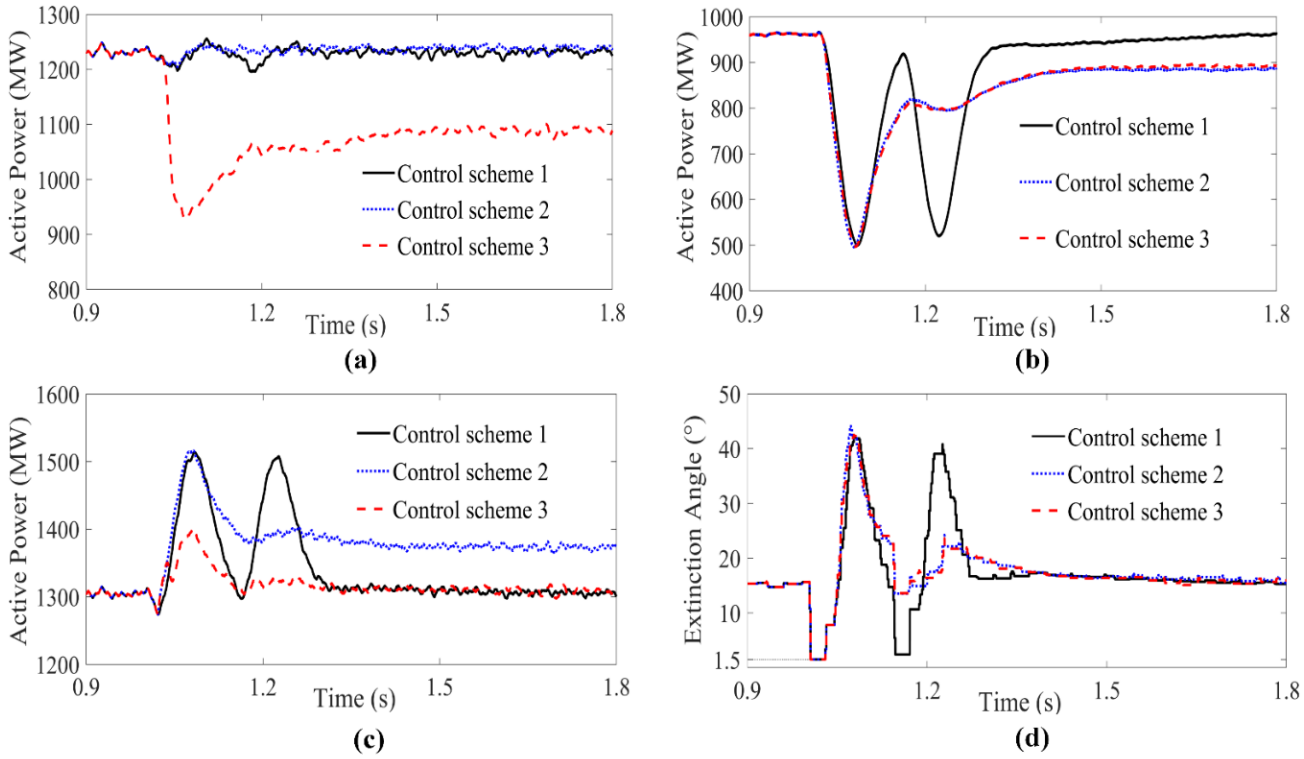

Figure 7. Simulation comparison of three control schemes: (**a**) active power output of wind farms; (**b**) active power transmission of HVDC system; (**c**) active power transmission of HVAC system; (**d**) extinction angle of HVDC inverter.

Control scheme 2 was adopted after the first CF occurred 20 ms, taking into account that data collection took 20 ms; thus, reactive power requirements of the HVDC system can be reduced and subsequent CFs can be effectively mitigated according to Equations (14)–(16). However, the active power output of the sending-end AC system does not change, and the active power of the HVDC system decreases, which will inevitably lead to the obvious overload phenomenon of the HVAC system in both transient and steady-state processes. The peak value of transient overload is similar to the peak value of overload phenomenon with control scheme 1, but the steady-state active power of the HVAC system increases by 8% after mitigating HVDC's subsequent CFs due to adjusting the HVDC active power transmission, and it is in the overload state for a long time, as shown in the blue curve in Figure 7c.

Control scheme 3 could be adopted considering the need to reduce the overload risk of the HVAC system while mitigating HVDC's subsequent CFs. Briefly, 20 ms after the first CF was detected, the active acceleration control of WTG and the pitch angle control of WTG were carried out according to Equations (18) and (19). WTGs are no longer in the MPPT output mode, and the active power output of wind farms is significantly reduced; the specific changes of electrical quantities in the system are shown in the red curve in Figure 7 after this control scheme was adopted. It can be seen that this control strategy can eliminate the steady-state power overload phenomenon of the HVAC system after the mitigation of HVDC's subsequent CFs, and the transient power shock of the HVAC system during the CF is reduced from 1520 MW to less than 1400 MW; thus, the possibility of tripping and other faults in the system is effectively reduced.

6.2. Actual Power Grid Simulation

With Power System Analysis Synthesis Program (PSASP), developed by China Electric Power Research Institute as a simulation tool, simulation analysis was carried out based on the actual power grid data in northwestern China. The HM area was selected as the

sending-end AC system, which contains high-proportion wind power and is connected with the HVDC system of TZ and the multi-circuit AC lines, including HD, HS, HT, etc.

The typical actual grid diagram simulated in this paper is shown in Figure 8. The HD line, which is the AC line from HM to DH, and the TZ line, which is the DC line from HM to ZZ, could be selected as the typical AC/DC transmission system, and since there are many wind farms in the HM area, the wind farm of YD was used as a typical wind farm in HM area for observation. In normal operation, power transmission of TZ monopile line is 3250 MW, power transmission of HD line is 700 MW, and the power output of wind farm of YD is 200 MW; the changes in each electrical quantity are shown in Figure 9.

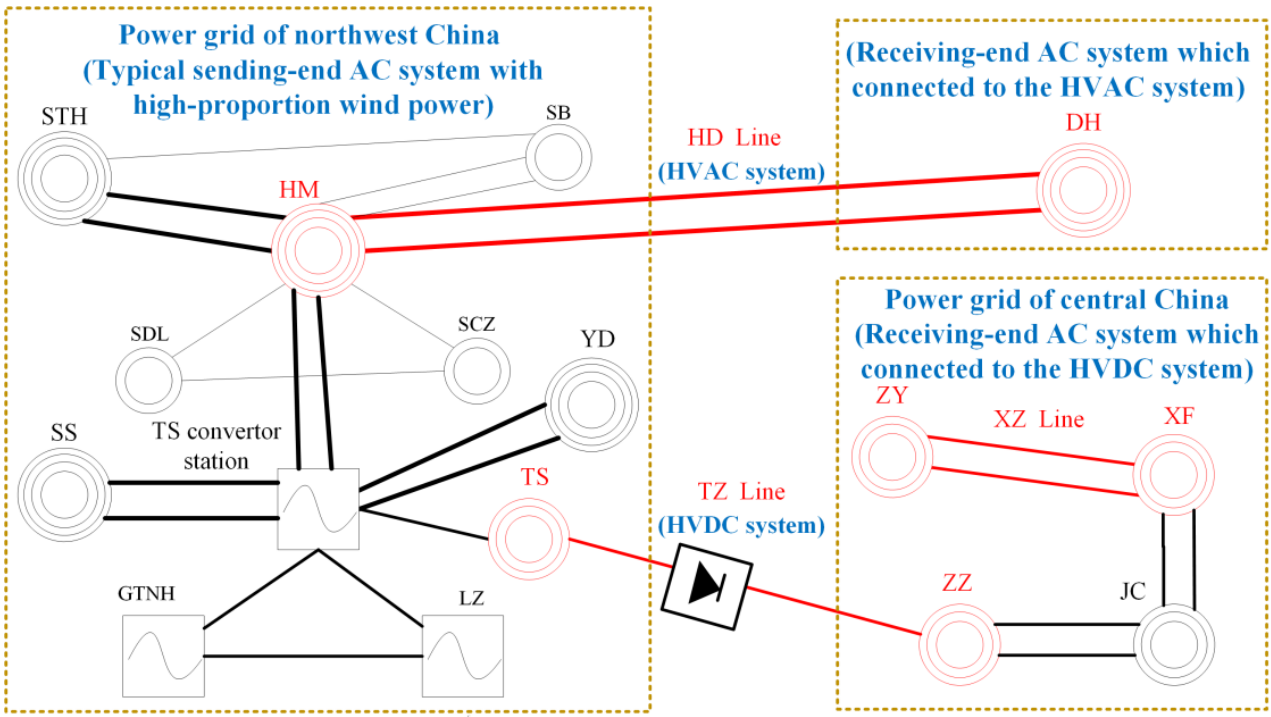

Figure 8. Typical actual grid diagram.

Set the XZ line, which is the AC line from XF to ZY with a voltage level of 500 kV in the AC system of the inverter side of the TZ line, to have a three-phase short circuit fault at 1 s. If control scheme 1 is adopted, the active power of the TZ line drops by 5250 MW twice due to the HVDC subsequent CFs, and the active power of the HD line connected with the TZ line also increases by 620 MW twice in succession in the transient process. The change in each electric quantity curve is shown in the black curve in Figure 9. The HVDC system is faced with locking risk caused by the subsequent CFs as well as transient and steady-state overload risk.

If control scheme 2 is adopted, the active power of the TZ line is reduced by adjusting the DC current command to reduce the corresponding reactive power demand, and the HVDC subsequent CFs can be mitigated at this time, as shown in the blue curve in Figure 9b. However, the HD line experiences transient and steady-state overload risk at this time, and the peak value of transient overload is similar to that in control scheme 1. The active power of the AC line increases by about 30% when the AC transmission line reaches a steady state, which will severely affect the safe and stable operation of the actual power grid, as shown in the blue curve in Figure 9c.

Control scheme 3 was adopted to reduce the power output of the energy base in northwestern China through the active control scheme of WTG while adjusting the active power of the TZ DC line. Taking the selected typical wind farm as an example, the active power output of the wind farms is reduced by 50% when the HD AC line is faced with overload risk; the active power output of the typical wind farm is shown in the red curve

in Figure 9a. According to the simulation comparison, the power shock on the AC line in the process of CF is effectively controlled, and the AC line steady-state overload risk is reduced, as is shown in the red curve in Figure 9c.

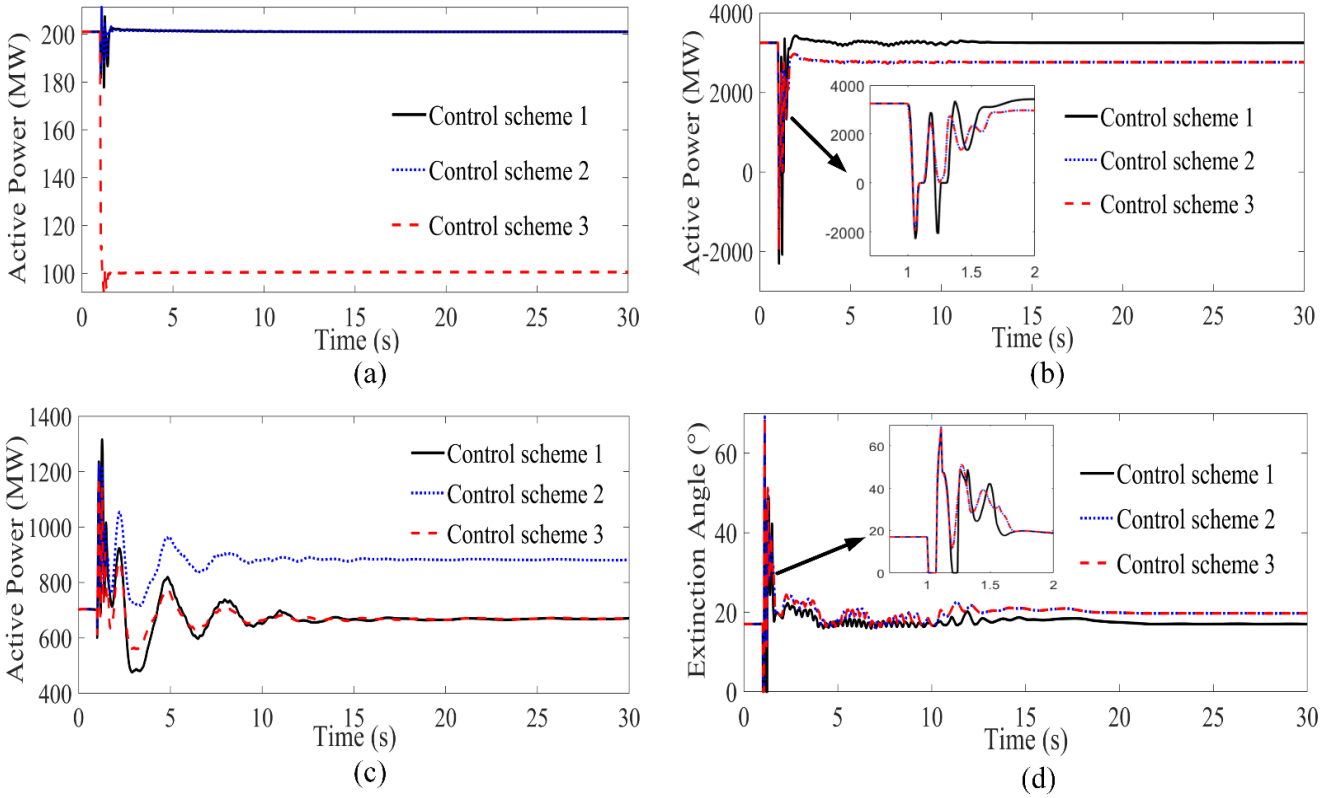

Figure 9. Simulation comparison of three control schemes in actual power grid: (**a**) active power output of YD wind farm; (**b**) active power of TZ line; (**c**) active power of HD line; (**d**) extinction angle of ZZ converter station.

7. Conclusions

HVDC's subsequent CFs of AC/DC transmission systems and the resulting large-scale power flow transfer were studied in this paper, to propose an active power coordinated control strategy of AC/DC transmission systems with high-proportion wind power. The proposed control scheme may be applied as a control strategy for the stability of future power systems to a certain extent, and the following conclusions can be obtained and extended based on the corresponding theory and simulation analysis:

(1) The AC-side fault of the HVDC system will cause subsequent CFs to occur in HVDC systems, resulting in a significant drop in the DC active power transmission in the AC/DC transmission system with high-proportion wind power, which causes large-scale power flow transfer. The factors that lead to HVDC subsequent CFs and overload phenomenon of the HVAC system were analyzed in this paper.

(2) An active power coordination control strategy was proposed for the AC/DC transmission system with high-proportion wind power considering the mitigation of subsequent CFs in the HVDC system; adjusting the DC current command to reduce the DC active power transmission can effectively reduce the reactive power demand during the HVDC-CF, so as to mitigate HVDC's subsequent CFs.

(3) HVDC-CF will cause the active power of the HVDC system to drop, and an overload phenomenon will occur in the adjacent HVAC system. The active power output of sending-end AC system with high-proportion wind power will be quickly reduced by the active acceleration control of WTG and the pitch angle control of WTG, according to the

proposed control scheme, which can reduce the transient power shock of the HVAC system during the process of HVDC-CF and keep the steady-state power transmission stable.

Author Contributions: Conceptualization, C.D. and J.D.; methodology, X.Z. and J.D.; software, C.D. and Y.H.; validation, Z.L., Z.Q. and X.Z.; formal analysis, F.X.; investigation, X.Z. and F.X.; resources, Z.L.; data curation, Y.H.; writing—original draft preparation, C.D. and Z.Q.; writing—review and editing, X.Z. and J.D.; visualization, C.D.; supervision, F.X.; funding acquisition, X.Z. All authors have read and agreed to the published version of the manuscript.

Funding: This research was funded by the Key Program of the National Natural Science Foundation of China, Grant Number 61933005.

Data Availability Statement: Data is contained within the article.

Conflicts of Interest: The authors declare no conflict of interest.

Appendix A

As regards Section 6.1 of this paper, the key parameters of the AC/DC transmission system model with high-proportion wind power built in PSCAD/EMTDC are shown in the following three tables: Table A1 is parameters of D-PMSG, Table A2 is LCC-HVDC system, and Table A3 is HVAC system.

Table A1. Parameters of D-PMSG.

Parameter	Value
Rated capacity	3 MW
Rated voltage	690 V
Wind speed	13 m/s
Stator resistance	0.0108 p.u.
Stator leakage reactance	0.102 p.u.
Rotor resistance	0.01 p.u.
Rotor reactance	0.11 p.u.
Inertia time constant	3 s

Table A2. Parameters of LCC-HVDC system.

Parameter	Value
Effective value of converter bus on inverter station	215.09 kV
Ideal no-load DC voltage at rectifier side	619.16 kV
Ideal no-load DC voltage at inverter side	277.63 kV
Equivalent commutation resistance at rectifier side	12.96 Ω
Equivalent commutation resistance at inverter side	25.54 Ω
DC resistance	5 Ω
Commutation reactance	13.3 Ω
Trigger angle	20°

Table A3. Parameters of HVAC system.

Parameter	Value
Voltage level	330 kV
Line length	200 km
Line resistance	0.12 Ω/km
Line inductance	2.05 mH/km

References

1. Moradi-Sepahvand, M.; Amraee, T. Transmission AC/DC Transmission Expansion Planning Considering HVAC to HVDC Conversion Under Renewable Penetration. *IEEE Trans. Power Syst.* **2021**, *36*, 579–591. [CrossRef]
2. Rehman, B.; ur Rehman, A.; Khan, W.A.; Sami, I.; Ro, J.-S. Operation and Challenges of Multi-Infeed LCC–HVDC System: Commutation Failure, AC/DC Power Flow, and Voltage Stability. *Appl. Sci.* **2021**, *11*, 8637. [CrossRef]
3. Liu, Z.; Zhang, Q. Study on the development mode of national grid of China. *Proc. CSEE* **2013**, *33*, 1–10.
4. Imdadullah; Alamri, B.; Hossain, M.A.; Asghar, M.S.J. Electric Power Network Interconnection: A Review on Current Status, Future Prospects and Research Direction. *Electronics* **2021**, *10*, 2179. [CrossRef]
5. Lotfjou, A.; Fu, Y.; Shahidehpour, M. Transmission AC/DC transmission expansion planning. *IEEE Trans. Power Syst.* **2012**, *27*, 1620–1628. [CrossRef]
6. Xu, Z.; Song, P.; Huang, H. Three macroscopic indices for describing the quality of AC/DC power grid structures. *IET Gener. Transm. Distrib.* **2016**, *10*, 175–182. [CrossRef]
7. Li, X.; Zhang, X.; Wu, L.; Lu, P.; Zhang, S. Transmission Line Overload Risk Assessment for Power Systems with Wind and Load-Power Generation Correlation. *IEEE Trans. Smart Grid.* **2015**, *6*, 1233–1242. [CrossRef]
8. Rahman, S.; Khan, I.; Alkhammash, H.I.; Nadeem, M.F. A Comparison Review on Transmission Mode for Onshore Integration of Offshore Wind Farms: HVDC or HVAC. *Electronics* **2021**, *10*, 1489. [CrossRef]
9. Mirsaeidi, S.; Dong, X.; Said, D.M. A Fault Current Limiting Approach for CF Prevention in LCC-HVDC Transmission Systems. *IEEE Trans. Power Deliv.* **2019**, *34*, 2018–2027. [CrossRef]
10. Lin, S.; Liu, J.; Liu, L.; Lei, Y.; Fu, C. A review of CF suppression methods for HVDC systems based on control protection measures. *Proc. CSEE* **2020**, *40*, 6045–6059.
11. Mirsaeidi, S.; Dong, X.; Tzelepis, D.; Mat, D. A predictive control strategy for mitigation of CF in LCC-based HVDC systems. *IEEE Trans. Power Electron.* **2019**, *34*, 160–172. [CrossRef]
12. Guo, C.; Li, C.; Liu, Y.; Jiang, B.; Zhao, C.; Zhou, Q. A DC current limitation control method based on virtual-resistance to mitigate the continuous CF for conventional HVDC. *Proc. CSEE* **2016**, *36*, 4930–4937.
13. Ni, X.; Zhao, C.; Guo, C.; Liu, H.; Liu, Y. Enhanced line commutated converter with embedded fully controlled sub-modules to mitigate CFs in high voltage direct current systems. *IET Power Electron.* **2016**, *9*, 198–206. [CrossRef]
14. Liu, L.; Lin, S.; Liao, K.; Sun, P.; Deng, Y.; Li, X.; He, Z. Extinction angle predictive control strategy for CF mitigation in HVDC systems considering voltage distortion. *IET Gener. Transm. Distrib.* **2019**, *13*, 5171–5179. [CrossRef]
15. Tang, Y.; Zheng, C.; Lou, B.; Hua, W.; Wang, L. Research on DC Power Control Strategy for Mitigating Continuous Commutation Failure. *Power System Technol.* **2019**, *43*, 3514–3521.
16. Ali, M.; Degefa, M.Z.; Humayun, M.; Safdarian, A.; Lehtonen, M. Increased Utilization of Wind Generation by Coordinating the Demand Response and Real-time Thermal Rating. *IEEE Trans. Power Syst.* **2016**, *31*, 3737–3746. [CrossRef]
17. Song, P.; Xu, Z.; Dong, H. UPFC-based line overload control for power system security enhancement. *IET Gener. Transmiss. Distrib.* **2017**, *11*, 3310–3317. [CrossRef]
18. Zhu, S.; Wang, T.; Wang, Z. Bi-level optimised emergency load/generator shedding strategy for AC/DC transmission system following DC blocking. *IET Gener. Transmiss. Distrib.* **2020**, *14*, 1491–1499. [CrossRef]
19. Tai, L.; Lin, M.; Wang, J.; Hou, C. Synchronous Control Strategy with Input Voltage Feedforward for a Four-Switch Buck-Boost Converter Used in a Variable-Speed PMSG Energy Storage System. *Electronics* **2021**, *10*, 2375. [CrossRef]
20. Mozayan, S.M.; Saad, M.; Vahedi, H.; Fortin-Blanchette, H.; Soltani, M. Sliding mode control of PMSG wind turbine based on enhanced exponential reaching law. *IEEE Trans. Ind. Electron.* **2016**, *63*, 6148–6159. [CrossRef]
21. Tiwari, R.; Krishnamurthy, K.; Neelakandan, R.B.; Padmanaban, S.; Wheeler, P.W. Neural Network Based Maximum Power Point Tracking Control with Quadratic Boost Converter for PMSG—Wind Energy Conversion System. *Electronics* **2018**, *7*, 20. [CrossRef]
22. Faruque, M.O.; Zhang, Y.; Dinavahi, V. Detailed modeling of CIGRE HVDC benchmark system using PSCAD/EMTDC and PSB/SIMULINK. *IEEE Trans. Power Deliv.* **2006**, *21*, 378–387. [CrossRef]